Optica Applicata, Vol. XXXI, No. 2, 2001

Design considerations for GaAs/(AlGa)As SCH and GRIN-SCH quantum-well laser structures. II. The results

TOMASZ CZYSZANOWSKI, MICHAŁ WASIAK, WŁODZIMIERZ NAKWASKI*

Institute of Physics, Technical University of Łódź, ul. Wólczańska 219, 93-005 Łódź, Poland.

A detailed optical model of complex multi-layered structures of the separate-confinement -heterostructure (SCH) lasers as well as graded-index (GRIN) SCH lasers presented in the first part of the paper is used to discuss some of the possible modifications of their structure to reduce room-temperature thresholds. Recommended design parameters have been found for each structure. Surprisingly, performance of relatively simple SCH lasers is found to be at least comparable with that of much more complex GRIN-SCH lasers.

1. Introduction

In the first part [1] of the paper, a detailed optical model of arsenide multi-layered separate-confinement-heterostructure (SCH) lasers has been presented. This approach is now used to discuss a possibility of optimizing their structures for the room-temperature low-threshold operation. Some structure modifications are also proposed and their impact on the performance of analyzed lasers is examined.

Although our model is quite comprehensive from an optical point of view, it does not contain an electrical part (see, *e.g.*, [2]–[8]), describing, among others, the current spreading effect, the injection of carriers into the active region, and, finally, the overbarrier current leakage. Conclusions following analysis of the above effects are, however, usually obvious, *e.g.*, resistivities of current paths should be as low as possible and definitely lower than those of surrounding areas, current leakage should be drastically reduced, carriers escaping from the active regions should be impeded, *etc.* But, anyway, electrical effects raise some limits to our purely optical considerations. These limits will also be taken into account when our final optimization suggestions are specified.

This part of the paper is organized as follows. An attempt to optimize the structure of SCH lasers is described in Section 2. Modifications of the structure of

* Also with the Center for High Technology Materials, University of New Mexico, Albuquerque, NM 87131, USA.

GRIN-SCH lasers are proposed in Section 3. The various SCH lasers are compared in Section 4, which is followed by conclusions.

2. The SCH lasers

The idea of the separate-confinement heterostructure was to create two different regions for recombining carriers (the active region) and for an optical field (the waveguide) to enable their separate optimization. But some construction parameters of the device should be still chosen as a result of various compromises. For example, the waveguide should be wide enough to reduce optical field penetration into cladding layers, but at the same time an increase in its thickness is followed by some reduction of the confinement factor Γ_{QW}, lowering the efficiency of coupling recombining carriers with the field (see Eq. (24) in [1]) and increasing the lasing threshold. Therefore, it is our intention to find in this section the recommended set of design parameters for the GaAs/(AlGa)As SCH lasers.

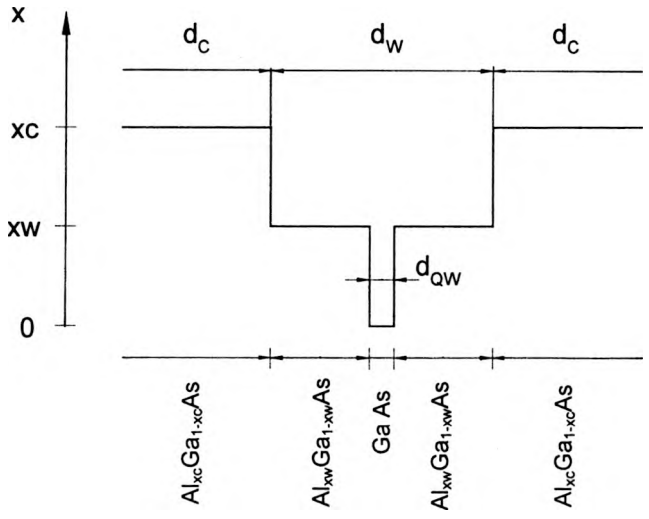

Fig. 1. Variation of the AlAs mole fraction in the SCH-SQW structure under consideration. Basic design parameters are also shown.

The typical SCH structure under consideration (Fig. 1) is composed of the SQW GaAs active layer placed in the very middle of the uniform $Al_{xw}Ga_{1-xw}As$ waveguide surrounded by two $Al_{xc}Ga_{1-xc}As$ claddings, where $xc > xw$. An impact of some changes of SCH design parameters on the device threshold is analyzed in following pictures. Figure 2a enables discussion of possible compositions of both cladding and waveguide layers, taking into account efficiency (Γ_{QW}) of coupling between an optical field and carriers. The curves were plotted for the typical (AlGa)As SCH-SQW of the 8-nm GaAs SQW active layer surrounded by two 0.12 μm $Al_{xw}Ga_{1-xw}As$ waveguide layers (so, $d_w = 0.248$ μm) and the

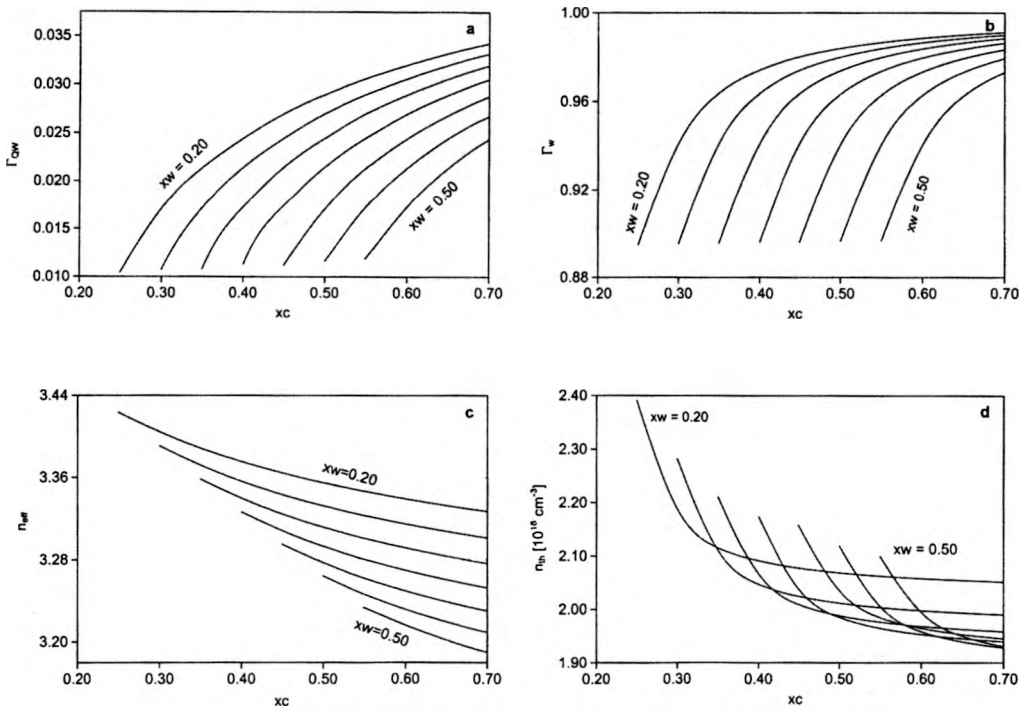

Fig. 2. Impact of the AlAs mole fractions in the waveguide xw and the cladding xc layers of the typical GaAs/(AlGa)As separate-confinement-heterostructure laser composing the 8-nm SQW active region and two 0.12 μm waveguide layers on: **a** – the RT confinement factor Γ_{QW} within the SQW GaAs active region, **b** – the RT confinement factor Γ_w within the waveguide, **c** – the RT effective index of refraction n_{eff}, and **d** – the RT threshold carrier concentration n_{th}. Successive curves are plotted for increasing AlAs mole fraction by 0.05 in the waveguide from $xw = 0.20$ up to $xw = 0.50$.

$Al_{xc}Ga_{1-xc}As$ cladding layers. As one can see, an increase in the AlAs mole fraction xc in cladding areas is followed by a considerable increase in the efficiency of optical field confinement within the SQW active layer Γ_{QW}. This confinement is more effective for lower AlAs mole fractions xw in the waveguide layers, because the step change of a refractive index at the waveguide/cladding boundary is proportional to the difference between AlAs mole fractions in both materials. Additionally, high $xc-xw$ values ensure low carrier leakage from the waveguide area. So, seemingly this difference should be chosen as high as possible. But, unfortunately, room-temperature (RT) electrical resistivities of both p-type and n-type $Al_xGa_{1-x}As$ materials are steadily increased with an initial increase in their AlAs mole fraction because both their carrier mobilities and carrier concentrations are then reduced (see, *e.g.*, [9]–[19]). Therefore, although an appropriate content step, $xc-xw > 0.3$, should still be preserved to prevent carrier leakage from the waveguide, both xc and xw should not be chosen too high.

The above confinement effect is even more pronounced in Fig. 2**b**, presenting analogous plots for the factor Γ_w describing efficiency of field confinement in the

whole waveguide containing the active layer. Analogously, Fig. 2c presents the lowering of the effective index of refraction n_{eff} (Eq. (16) in [1]) with an increase in both xw and xc. This decrease is mostly a result of steadily reduced refractive indices of the waveguide and the cladding materials, because the index of refraction of $Al_xGa_{1-x}As$ is monothonically decreased with an increase in x. The most interesting plots for the SCH structure are, however, shown in Fig. 2d, presenting threshold carrier concentrations n_{th} versus xc (AlAs mole fraction in the claddings) for various xw (AlAs mole fraction in the waveguide). We limit our threshold considerations to the determination of n_{th} only because the threshold current density j_{th} is directly related to n_{th} with the aid of Eq. (25) in [1]. It is known from Figs 2a and b, that, in the whole xc range, both confinement factors Γ_{QW} and Γ_w exhibit the highest values for relatively low $xw = 0.2$. Lower thresholds are, however, found in Fig. 2d to be achieved for higher xw values, because then the band-to-band absorption α_{bb} in the waveguide is lower (*c.f.*, Eq. (22) in [1]). Therefore an optimal xw value seems to be equal to about 0.3, since its further increase reduces n_{th} much slower and is additionally very inappropriate because of the above mentioned increase in an electrical resistivity (RT electrical resistivity of $Al_{0.4}Ga_{0.6}As$ is about 5 times higher than that of $Al_{0.3}Ga_{0.7}As$ [13]). For the above value of $xw = 0.3$, a recommended xc value should be higher than 0.6, *e.g.*, $xc = 0.7$, to reduce the carrier leakage. It should be additionally stressed that further increase (over $x \approx 0.4$) in the AlAs mole fraction of $Al_xGa_{1-x}As$ materials is followed by a steady slow decrease in their RT electrical resistivities [13].

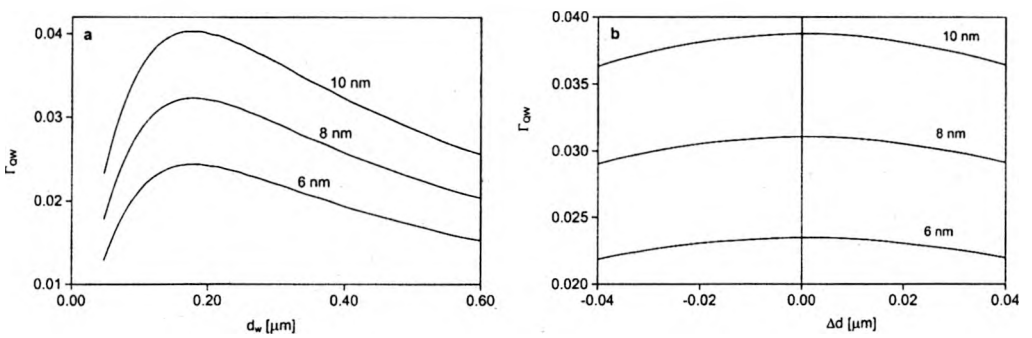

Fig. 3. The RT confinement Γ_{QW} factor in the typical SCH laser (the GaAs SQW active layer (of a given thickness d_{QW}) inside the $Al_{0.3}Ga_{0.7}As$ waveguide) versus: a – the waveguide width d_W for different SQW widths d_{QW}, b – displacement Δd of the GaAs SQW active layer from its central position towards the n-cladding.

Let us now consider an influence of the waveguide width d_W on laser threshold properties. To obtain high Γ_{QW} values, d_W should not be too thin because then the optical field will penetrate both the n- and p-type claddings to an unaccepted extent. On the other hand, however, it should not be too thick either, because then a smaller part of the field will interact with carriers inside an active region, so the confinement factor Γ_{QW} will be reduced. Therefore, there exists an optimal

waveguide width equal in our case (*cf.*, Fig. 3**a**) to about $d_W = 160$ nm, disregarding the width d_{QW} (6 nm, 8 nm or 10 nm) of the SQW. It should, however, be remembered that, for some applications, the width of the waveguide is chosen to obtain a desired far-field pattern rather than a minimum threshold.

An impact of the width d_C of cladding layers on lasing threshold was also examined. It was found that both claddings should be at least 0.7−0.8 μm wide, *e.g.*, $d_C = 1$ μm, to protect laser radiation from penetration lossy regions. Their further increase practically does not improve confinement of an optical field. From the electrical point of view, on the other hand, relatively high-resistive cladding layers should be as narrow as possible, so the above value may be regarded as a lower limit of their widths.

An important question in device technology concerns the necessary level of precise device manufacturing, *i.e.*, what changes of construction parameters with respect to their optimal values are still acceptable. One of the most essential problems in manufacturing SCH-SQW structures is, for example, a precise location of their single quantum wells at the very middle point of waveguides. As expected, Fig. 3**b** presents a considerable decrease in the confinement factor Γ_{QW} when the active region is shifted by Δd from its recommended central position in the SCH laser of 8-nm GaAs SQW placed in the 0.168 μm $Al_{0.3}Ga_{0.7}As$ waveguide. The plot may help to acquaint oneself with possible consequences of an unwanted shift of the SQW active layer. Concluding, let us, however, state that very exact calculations revealed an interesting fact that, unexpectedly, to minimize threshold currents, more favourable is a somewhat nonsymmetrical structure, in which the SQW is shifted from its central position by 5−7 nm towards the n-type cladding (*i.e.*, for positive Δd in Fig. 3**b**). The above fact is connected with higher optical losses in p-type than in n-type claddings, but this effect is practically nearly insignificant.

Table 1. Recommended values of basic design parameters of the GaAs/(AlGa)As SCH-SQW lasers for their RT low-threshold operation.

Parameter	Notation	Value
AlAs mole fraction in the waveguide	xw	0.30
AlAs mole fraction in the claddings	xc	0.70
Waveguide thickness	d_W	160 nm
Cladding thickness	d_C	1 μm

Using our approach developed in Section 2 of [1], we have found in this section recommended values of basic design parameters of the GaAs/(AlGa)As SCH lasers for their low-threshold RT operation. They are listed in Table 1.

3. The GRIN-SCH lasers

Two modified versions of the GRIN-SCH-SQW structure under consideration are proposed in Fig. 4. In the first design (Fig. 4**a**), uniform $Al_{0.3}Ga_{0.7}As$ layers of

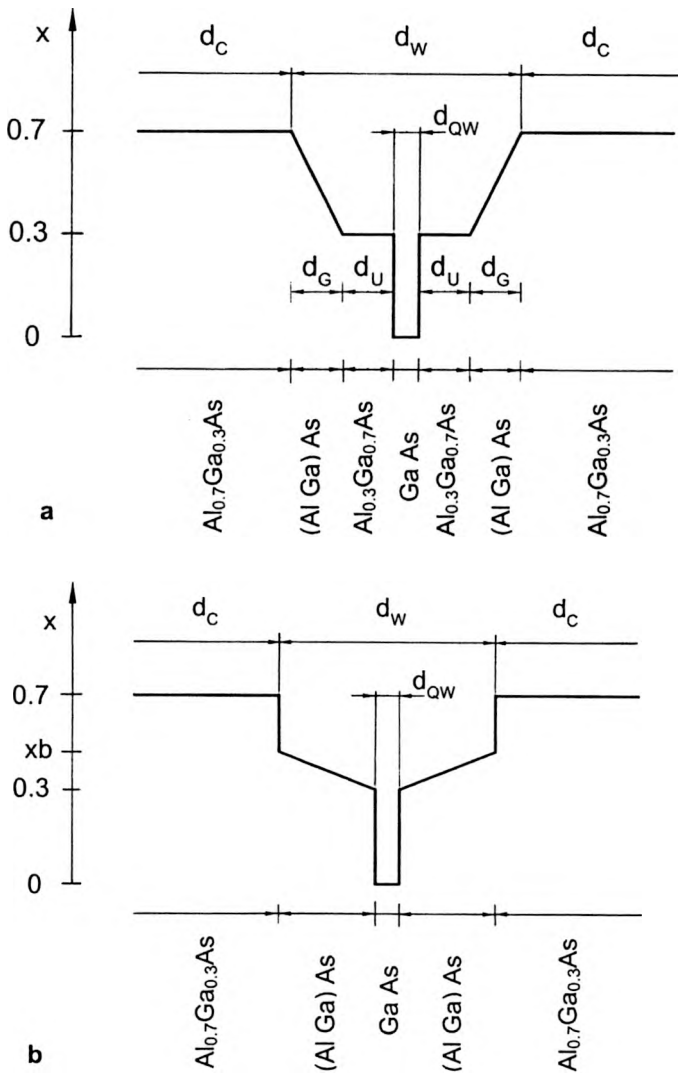

Fig. 4. Variation of the AlAs mole fraction in the modified GRIN-SCH-SQW structures under consideration. The first device (**a**) is reduced to the standard GRIN-SCH-SQW structure and to the SCH-SQW structure for $d_U = 0$ and $d_G = 0$, respectively. Various forms (from linear to parabolic) of a change of an AlAs content within the graded layers are considered. The second design (**b**) becomes the standard GRIN-SCH-SQW structure for $xb = xc = 0.7$, whereas for $xb = 0.3$, it is reduced to the SCH-SQW structure.

thicknesses d_U are placed on both sides of the SQW active layer followed by graded (AlGa)As layers of thicknesses d_G. A composition of the uniform layers, as well as composition of the 2-μm $Al_{0.7}Ga_{0.3}As$ cladding layers, are chosen on the basis of earlier analysis of the SCH-SQW GaAs/(AlGa)As structure in Section 2. As one can see, this modified design is reduced to the standard GRIN-SCH-SQW structure for

$d_U = 0$ (*cf.*, Fig. 1e in [1]), whereas, for $d_G = 0$, the simpler SCH-SQW structure is obtained (*cf.*, Fig. 1d in [1]). In this section, an influence of both the d_U thicknesses of uniform parts of the waveguide and the d_G thicknesses of its graded parts on lasing thresholds of the modified GRIN-SCH-SQW devices is examined. Additionally, various forms of an AlAs change Δx in graded layers

$$\Delta x \propto (x - x_G)^k \tag{1}$$

are discussed. In Eq. (1), x_G stands for the coordinate of a starting point of the graded layer and exponent k may be changed from 1 (linear grading) to 2 (parabolic grading).

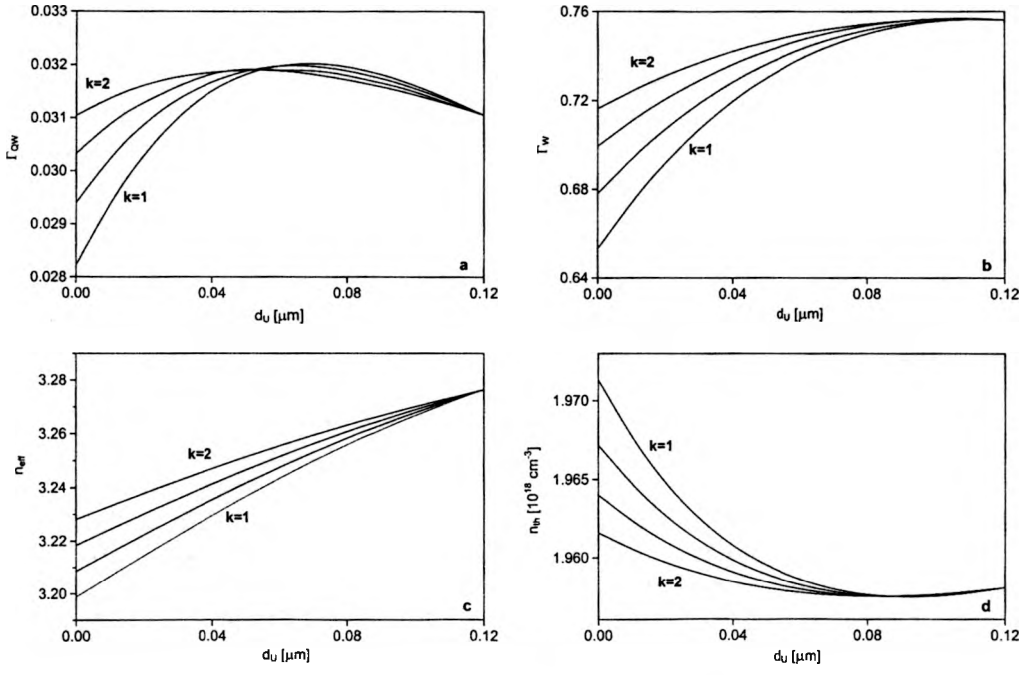

Fig. 5. Impact of the thickness d_U of a uniform part of the waveguide (*cf.*, Fig. 4**a**) of the first modified GRIN-SCH-SQW laser ($d_C = 2$ μm, $d_{QW} = 8$ nm and $d_W = 0.248$ μm) on: **a** — the RT confinement factor Γ_{QW} within the SQW active layer, **b** — the RT confinement factor Γ_W within the waveguide, **c** — the RT effective index of refraction, and **d** — the RT threshold carrier concentration. Successive curves are plotted for $k = 1$, 5/4, 11/7, and 2.

Figure 5 illustrates an impact of the d_U thickness on some parameters of the modified GRIN-SCH-SQW laser with $d_C = 2$ μm, $d_{QW} = 8$ nm, and constant $d_W = 0.248$ mm, *i.e.*, for $d_U + d_G = 120$ nm. Edge points of these plots correspond to the standard GRIN-SCH-SQW structure (for $d_U = 0$ nm) and to the SCH-SQW structure (for $d_U = 120$ nm). A dependence of the confinement Γ_{QW} factor on d_U is,

Table 2. Recommended values of basic design parameters of the standard GaAs/(AlGa)As GRIN-SCH-SQW lasers for their RT low threshold operation.

Parameter	Notation	Value
Waveguide thickness (linear grading)	d_W	350 nm
Waveguide thickness (parabolic grading)	d_W	270 nm
AlAs mole fraction in the claddings	x_C	0.70

for example, shown in Fig. 5**a**. As one can see, structures with $d_U \approx 0.07$ μm exhibit in this case the highest Γ_{QW} values. They are increased by as much as over 13% (*i.e*,. from 0.0282 to 0.0320) with respect to the standard GRIN-SCH-SQW structure ($d_U = 0$) with a linear ($k = 1$) profile of the AlAs mole fraction in graded layers. From the figure, some additional conclusions concerning recommended grading may be deduced. First of all, parabolic grading ($k = 2$) is found to ensure better field confinement within the SQW active layer than the linear one in the case of the standard structure ($d_U = 0$). In the modified structure, however, linear grading enables obtaining somewhat better results. To achieve maximal Γ_{QW} values, thicker d_U layers should be applied for decreasing exponents k (*cf.* Eq. (1)) in graded layers.

The above conclusions are confirmed in Fig. 5**b**, in which plots of the Γ_W (field confinement within the whole waveguide containing the active layer) versus d_U are shown. Again, parabolically graded layers ensure the best field confinement in the case of the standard GRIN-SCH device version and an increase in d_U enables additional increase in Γ_W in the modified structure. An effective index of refraction is also increasing with an increase in d_U (Fig. 5**c**) because of a better field confinement within the waveguide (*cf.* Fig. 5**b**) of higher refractive index than that of claddings.

Plots of threshold carrier concentration versus d_U are shown in Fig. 5**d**. Parabolic grading turns out to reduce lasing threshold in the standard GRIN-SCH-SQW laser ($d_U = 0$) with respect to a linear one. Further improvement may be achieved using the modified version of this device with $d_U \approx 0.09$ μm. In the last case, a form of a gradual change of the AlAs mole fraction in graded layers is practically unimportant. It is interesting to note that the optimal d_U value, ensuring the lowest lasing threshold, is found to be somewhat larger than that giving the highest Γ_{QW} value (*cf.* Fig. 5**a**). This effect is caused by a better field confinement within the waveguide (*cf.* Fig. 5**b**). Surprisingly, the simple SCH-SQW structure ($d_U = 120$ nm) is found in this case to exhibit lower threshold than the standard ($d_U = 0$) GRIN-SCH-SQW structure. It should, however, be remembered that the GRIN structure produces additionally an electric field increasing the efficiency of carriers collected within a thin SQW active layer [20]. The above effect is not included in our model. Therefore, the GRIN structure may considerably improve lasing performance of the SCH devices.

Figure 6 presents another comparison of the first modified GRIN-SCH-SQW structure (Fig. 4**a**) with linear grading ($k = 1$) equipped with waveguides of various

widths d_W. Each curve starts for $d_G = 0$ from the SCH-SQW structure ($d_W = 2d_U + d_{QW}$) and ends for $d_U = 0$ ($d_W = 2d_G + d_{QW}$), *i.e.*, for the standard GRIN-SCH-SQW structure. The most interesting plots are presented this time in Fig. 6**a**, showing, for each d_W, the d_G dependence of the confinement factor Γ_{QW}. Initially, for relatively thin waveguides, the best coupling between carriers and an optical field, *i.e.*, the highest Γ_{QW} values, are always achieved for the simple SCH-SQW structures (*i.e.*, for $d_G = 0$). The standard GRIN-SCH-SQW structures ($d_U = 0$) then seem to be definitely the worst solution. For steadily thicker

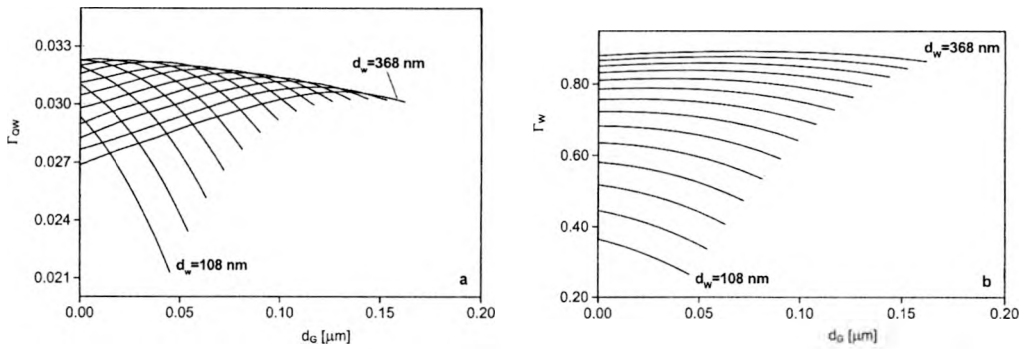

Fig. 6. Impact of the thickness d_G of a linearly graded part of the waveguide (*cf*, Fig. 4**a**) of the first modified GRIN-SCH-SQW laser ($d_C = 2$ μm and $d_{QW} = 8$ nm) on: **a** – the RT confinement factor Γ_{QW} within the SQW active layer, and **b** – the RT confinement factor Γ_W within the waveguide. Successive curves are plotted for the waveguide thicknesses d_W ($= 2d_G + 2d_U + d_{QW}$) changing by 20 nm from $d_W = 108$ nm up to $d_W = 368$ nm.

waveguides, starting with $d_W = 168$ nm, two interesting behaviours are observed. First of all, the modified GRIN-SCH-SQW structures of increasing thicknesses d_G of a graded part of the waveguide are becoming the devices with the best coupling. Next, this d_G value is becoming less and less critical as regards to the Γ_{QW} value. Anyway, the highest Γ_{QW} value is achieved in this case for $d_W = 188$ nm, $d_G = 20$ nm and $d_U = 70$ nm. Those values are chosen as recommended design parameters of the first modified GRIN-SCH-SQW lasers (Tab. 3). An increase in the waveguide thickness d_W considerably improves the efficiency of the field confinement within the waveguide, which is seen in Fig. 6**b**. Unfortunately, at the same time, efficiency of the carriers capturing in the SQW active layers is steadily reduced which is not included in our model. Therefore high Γ_{QW} values should be treated as better quality factors in SCH lasers than the Γ_W ones.

Figure 7 presents some results (plots of Γ_{QW} versus d_W for various xb) obtained for the second modified GRIN-SCH-SQW structure shown in Fig. 4**b**. The structure is reduced to the standard GRIN-SCH-SQW structure and to the SCH-SQW structure for $xb = xc$ and $xb = 0.3$, respectively. It may be seen in the figure that for relatively thin waveguides, higher steps $xc - xb$ at their edges ensure better field confinement, whereas, in thicker waveguides, standard GRIN-SCH-SQW structure

Table 3. Recommended values of basic design parameters of the first modified GaAs/(AlGa)As GRIN-SCH-SQW lasers (Fig. 4a) for their RT low-threshold operation.

Parameter	Notation	Value
Waveguide thickness	d_W	188 nm
Thickness of the graded part of the waveguide	d_G	20 nm
Thickness of the uniform part of the waveguide	d_U	70 nm
AlAs mole fraction in the claddings	xc	0.70
AlAs mole fraction in the uniform part of the waveguide	xu	0.30

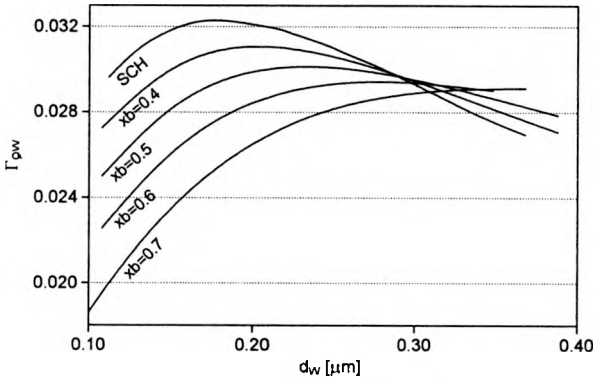

Fig. 7. Impact of the waveguide width d_W in the second modified GRIN-SCH-SQW structure (Fig. 4b) on the RT confinement factor Γ_{QW} within its SQW active layer for various steps $xc-xb$ of the AlAs modefraction at the waveguide edges. In the calculations, the $Al_{0.7}Ga_{0.3}As$ cladding layers are assumed.

($xb = xc = 0.7$) becomes more appropriate. Nevertheless, the first modified GRIN -SCH-SQW structure (Fig. 4a) seems to be more promising.

4. Comparison between various SCH structures

Let us first compare the SCH-SQW structure with the standard ($d_U = 0$) GRIN -SCH-SQW structures equipped with linear or parabolic gradings. The results are illustrated in Fig. 8. For $d_W = 0.248$ μm, values given in Fig. 8 are identical with those obtained from Fig. 5 for $d_U = 0$. As previously in Fig. 6, it is evident from Fig. 8 that for relatively narrow waveguides, the simple SCH-SQW structure may ensure better field confinements than the structure with graded interfaces. However, taking additionally into account the collecting of carriers within the SQW active layer, which is definitely more efficient in GRIN structures [20], thresholds of these more advanced devices are expected to be lower than those of the above simple SCH devices. Nevertheless, it should be noted that optimal d_W values (see Tab. 2) are in the case of standard GRIN structures (for which they are equal to about 0.27 μm and 0.35 μm for parabolic and linear gradings, respectively) considerably

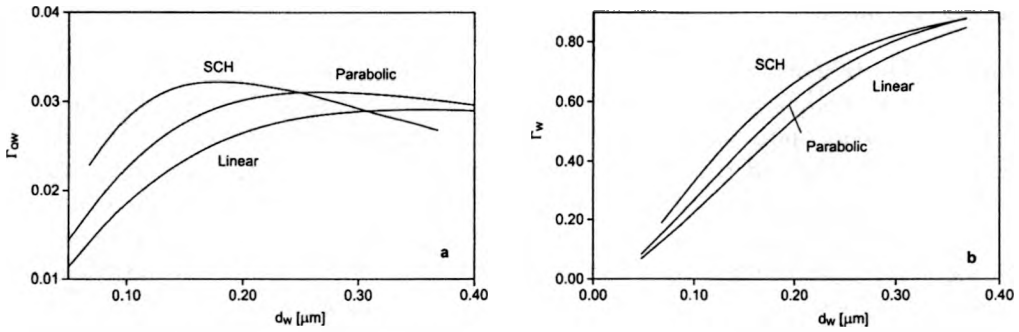

Fig. 8. Comparison between the SCH-SQW structure and the standard GRIN-SCH-SQW structure ($d_U = 0$) with both the linear and parabolic gradings (*cf.* Fig. 1) presenting dependences on the waveguide thickness d_W of: **a** – confinement factor Γ_{QW}, and **b** – confinement factor Γ_W, both for $d_{QW} = 8$ nm.

higher than that for the SCH structure (*cf.* Tab. 1). It is also worthwhile to notice that the parabolic grading usually ensures better confinement than the linear one.

Analogous comparison between the SCH-SQW structure and the first modified (assuming $d_U = 0.03$ μm) GRIN-SCH-SQW structure (Fig. 4**a**) with both linear and parabolic grading is shown in Fig. 9. As previously, the plots present dependences on

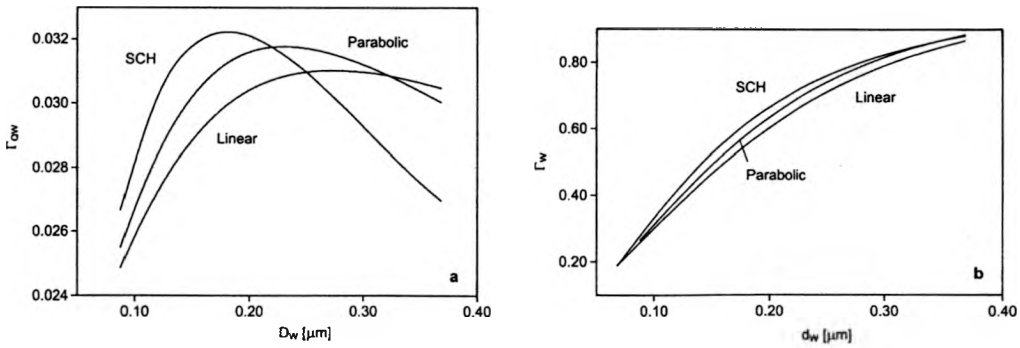

Fig. 9. Comparison between the SCH-SQW structure and the first modified GRIN-SCH-SQW structure ($d_U = 0.03$ μm) with both the linear and parabolic gradings (*cf.* Fig. 4**a**) presenting dependences on the waveguide thickness d_W of: **a** – confinement factor Γ_{QW}, and **b** – confinement factor Γ_W, both for $d_{QW} = 8$ nm.

the waveguide thickness d_W of both the field confinement factor Γ_{QW} within the SQW active layer (Fig. 9**a**) and the analogous factor Γ_W for the field confinement within the whole waveguide (Fig. 9**b**). Curves plotted for the SCH-SQW structure are identical with those shown in Fig. 8. As one can see, an additional degree of freedom (the thickness d_U of a uniform part of the waveguide) enables better than previously field confinement within the SQW active layer. Therefore, this design seems to be more promising as a low-threshold RT laser device than the standard one.

5. Conclusions

Various GaAs/(AlGa)As separate-confinement-heterostructure lasers, *i.e.*, simple SCH ones as well as standard and modified GRIN-SCH ones, have been examined using a detailed optical modeling to discuss an impact of their design parameters on their low-threshold room-temperature operation. For all three versions of the SCH lasers, recommended design parameters have been determined. Surprisingly, from an optical point of view considered in this paper, performance of a relatively simple SCH structure has been found to be at least comparable with much more complex GRIN structures. This conclusion is in agreement with observed properties of both the above SCH structures [21]. The modified GRIN-SCH design (Fig. 4a) with its additional degree of freedom of construction enables more advanced modeling of an optical-field profile within the laser structure.

Acknowledgements — This work was supported by the Polish State Committee for Scientific Research (KBN), grants No. 8-T11B-018-12, 7-T11B-073-21, and by the US–Poland Maria Sklodowska-Curie Joint Fund No. MEN/NSF-98-336.

References

[1] CZYSZANOWSKI T., WASIAK M., NAKWASKI W., Opt. Appl. **31** (2001), 313.
[2] CHINN S.R., ZORY P.S., REISINGER A.R., IEEE J. Quantum Electron. **24** (1988), 2191.
[3] WENZEL H., WUNSCHE H.-J., Phys. Stat. Sol. A **120** (1990), 661.
[4] LI Z.-H., DZURKO K.M., DELAGE A., MCALISTER S.P., IEEE J. Quantum Electron. **28** (1992), 792.
[5] TSAI CHIN-YI, TSAI CHIN-YAO LO Y.-H, EASTMAN L.F., IEEE Photon. Technol. Lett. **7** (1995), 599.
[6] TSUCHIYA H., MIYOSHI T., IEEE J. Quantum Electron. **32** (1996), 865.
[7] BUGAJSKI M., KANIEWSKA M., REGIŃSKI K., *et al.*, Proc. SPIE **3186** (1997), 310.
[8] KURAKAKE H., J. Appl. Phys. **84** (1998), 5643.
[9] NEUMANN H., FLOHRER U., Phys. Stat. Sol. A **25** (1974), K145.
[10] SPRINGTHORPE A.J., KING F.D., BECKE A., J. Electron. Mat. **4** (1975), 101.
[11] MUKAI S., MAKITA Y., GONDA S., J. Appl. Phys. **50** (1979), 1304.
[12] STRINGFELLOW G.B., J. Appl. Phys. **50** (1979), 4178.
[13] LEE H.J., JURAVEL L.Y., WOOLLEY J.C., SPRINGTHORPE A.J., Phys. Rev. B **21** (1980), 659.
[14] MASU K., KONAGAI M., TAKAHASHI K., J. Appl. Phys. **51** (1980), 1060.
[15] YANG J.J., MOUDY L.A., SIMPSON W.I., Appl. Phys. Lett. **40** (1982), 244.
[16] ISHIKAWA T., SAITO J., SASA S., HIYAMIZU S., Jpn. J. Appl. Phys. **21** (1982,) L675.
[17] SALMON L.G., DHAENES I.J., J. Vac. Sci. Technol. B **2** (1984), 197.
[18] BHATTACHARYA P.K., DAS U., LUDOWISE M.J., Phys. Rev. B **29** (1984) 6623.
[19] SUN S.Z., ARMOUR E.A., ZHENG K., SCHAUS C.F., J. Cryst. Growth **113** (1991), 103.
[20] HERSEE S., BALDY M., ASSENAT P., DE CREMOUX B., DUCHEMIN J.P., Electron. Lett. **18** (1982), 618.
[21] BUGAJSKI M., private communication.

Received October 9, 2000